Available online at www.sciencedirect.com
ScienceDirect
Journal of Molecular Catalysis A: Chemical 264 (2007) 179–191
JOURNAL OF MOLECULAR CATALYSIS A: CHEMICAL
www.elsevier.com/locate/molcata

Insight into Friedel-Crafts acylation of 1,4-dimethoxybenzene to 2,5-dimethoxyacetophenone catalysed by solid acids—mechanism, kinetics and remedies for deactivation

Ganapati D. Yadav *, Ketan P. Pimparkar

Department of Chemical Engineering, University Institute of Chemical Technology, University of Mumbai, Matunga, Mumbai 400 019, India

Received 22 May 2006; received in revised form 22 July 2006; accepted 24 July 2006
Available online 19 October 2006

Abstract

Friedel-Crafts acylation of aromatic ethers is challenging, which frequently encounters rapid catalyst deactivation by the ether. Although H-Y and H-β are known to perform better, there is still deactivation due to both the ether and the acylated ether. In the current work, the synthesis of 2,5-dimethoxyacetophenone, an intermediate used in the production of fine chemicals, was carried out via acylation of 1,4-dimethoxybenzene with acetic anhydride over various solid acid catalysts such as sulfated zirconia, UDCaT-1, UDCaT-5, 20% w/w $H_3P_{12}W_{40}$/K10, 20% w/w $Cs_{2.5}H_{0.5}P_{12}W_{40}$/K10, Amberlyst-15 and Indion-125. The cation exchange resins, Amberlyst-15 and Indion-125, were superior to other inorganic solid acids. A systematic study was undertaken to understand the reaction mechanism and catalyst functioning with Indion-125. The catalyst gets deactivated slowly over repeated use and this was studied independently. The adsorption of reactants and products was studied from pure component solutions and mixtures. The experimental data so generated were used to develop a model, incorporating deactivation. The model fits the experimental data very well. The current work gives an insight into choice of catalyst, kinetic modeling, studies in catalyst deactivation and methods to avoid deactivation.

Keywords: Friedel-Crafts acylation; 1,4-Dimethoxybenzene; 2,5-Dimethoxyacetophenone; Acetic anhydride; Sulfated zirconia; Heteropoly acids; $H_3P_{12}W_{40}$; $Cs_{2.5}H_{0.5}P_{12}W_{40}$; Acid treated clay; Montmorillonite clay; Mesoporous solid superacids; UDCaT-1; UDCaT-5; Amberlyst-15; Indion-125; Deactivation; Dynamic adsorption; Kinetics; Mechanism

1. Introduction

Acid catalyzed Friedel-Crafts acylation constitutes a major route to synthesize aromatic ketones, which are valuable precursors in dyestuff, agrochemicals, fine chemicals and pharmaceuticals industries. Traditionally homogeneous catalysts are used including Bronsted acids (sulphuric acid, polyphosphoric acid, hydrofluoric acid) or Lewis acids ($AlCl_3$, $ZnCl_2$ and BF_3 in nitrobenzene, carbon disulfide and dichloromethane) [1,2]. These catalysts are often required in little over stoichiometric amounts for acylations and selectivity to the desired ketone is poor. Besides, the post treatment of the reaction mass leads to generation of huge quantities of deleterious waste. Additionally the corrosive nature of acids leads to increasing costs due to premature ageing of the processing equipment and pipe lines. The acylating agents used in most of the traditional processes are the expensive and polluting acyl halides that require special care in handling and work up. With the increasing emphasis on green chemistry and technology, efforts have been made to develop environmentally friendly yet cost efficient processes for the synthesis of aromatic ketones. A plethora of solid acids has been tested to replace homogeneous acid catalysts by several researchers all over the world, and obviously zeolites are the most widely studied owing to their ease of preparation and/or availability, robustness and commercial success in refinery technologies. Solid acid catalysts are easy to recover and reuse, produce no salts, overcome corrosion problems thereby allowing use of cheaper materials of construction; they permit the use of cheaper and non polluting carboxylic acids and anhydrides as acylating agents, and offer several different reactor config-

* Corresponding author. Tel.: +91 22 2410 2121; fax: +91 22 2414 5614.
E-mail addresses: gdyadav@yahoo.com, gdyadav@udct.org (G.D. Yadav).

1381-1169/$ – see front matter © 2006 Elsevier B.V. All rights reserved.
doi:10.1016/j.molcata.2006.07.075

Nomenclature

a	activity of the catalyst
a_p	external surface area per unit liquid volume (cm^2/cm^3)
A	1,4-dimethoxybenzene
B	acetic anhydride
C	acetic acid
C_s	concentration of active sites on the catalyst surface (mol/g)
C_t	total concentration of active sites (mol/g)
C_A	concentration of A in the liquid phase (mol/cm^3)
C_{AL}	concentration of species A in the liquid phase at any time t (mol/cm^3)
C_{BS}	concentration of acetic anhydride on the catalyst surface
C_{CS}	concentration of acetic acid on the catalyst surface
C_{ALi}	initial concentration of species A in the liquid (mol/cm^3)
C_{ALf}	final concentration of species A in the liquid phase at infinite time
C_{MS}	concentration of 2,5-dimethoxybenzene on the catalyst surface
D	2,5-dimethoxyacetophenone
k_{ad}	adsorption constant (cm^3/(g cat/s))
k_A	adsorption constant per unit active site of catalyst
k_A	adsorption constant ($k_{ad}C_t$)
k_{DE}	deactivation rate constant
k_{SL}	solid–liquid mass transfer coefficient (cm/s)
k_{SR}	reaction rate constant assuming only forward reaction
k_{D1}	desorption constant for D_1
k_{D2}	desorption constant for D_2
k'_{D1}	desorption constant for D_1
k'_{D2}	desorption constant for D_2
K_A	adsorption equilibrium constant for A
K'_A	adsorption equilibrium constant for A, cm^3/gm ($=K_AC_t$)
K_{A1}	adsorption equilibrium constant for D
K_{A2}	adsorption equilibrium constant for C
K_{D1}	desorption equilibrium constant for D ($K_{D1} = k_{D1}/k'_{D1}$)
K_{D2}	desorption equilibrium constant for $C = k_{D2}/k'_{D2}$
M	2,5-dimethoxyacetophenone
M	initial mole ratio of acetic anhydride to 1,4-dimethoxybenzene (in Table 1) and Eq. (37) onwards
S_A	surface concentration of adsorbed A (mol/g)
w	catalyst loading, g/cm^3 of liquid

urations. Thus, solid acid catalysts can advantageously replace conventional catalysts.

Acylations are very difficult to accomplish with substituted benzenes using solid acids. In the case of acylation of aromatic ethers, indeed it is a formidable task, due to rapid deactivation

Table 1
Best fit values for Eq. (38) using nonlinear regression in Polymath 5.1

T (°C)	$k_{SR\times10^2}$	K_A	k_{DE}	K_{A1}	K_{A2}	R^2
90	3.60	1400	0.01	1000	1000	0.9795
95	5.00	1250	0.0105	800	833.33	0.9939
100	14.0	985.6	0.02	684.931	657.89	0.9716
105	16.0	755	0.0203	546.44	537.63	0.9844
$M=1$	9.50	1056	0.019	724.63	675.67	0.9866

$M=1$ implies reaction at molar ratio of reactants equal to unity. Where A: 1,4-dimethoxybenzene, B: acetic anhydride, C: acetic acid, D: 2,5-dimethoxyacetophenone, k_{SR} is reaction rate constant assuming only forward reaction, K_A is the adsorption equilibrium constant for B, k_{DE} is the deactivation rate constant, K_{A1} is the adsorption equilibrium constant for D, K_{A2} is the adsorption equilibrium constant for C.

of the catalysts, related to strong adsorption of reactants or products and intra-particle diffusion limitation. Zeolite HY and Hβ in chlorobenzene have been used for acylation of aromatic ethers at higher temperatures but still deactivation of the catalyst occurs rapidly due to the saturation of the active sites by the products acetic acid and/or the acylated product [3–7]. As an alternative to zeolites, several acylations of substituted benzenes were investigated with a variety of catalysts in our laboratory, including sulfated zirconia, UDCaT-1, UDCaT-5, dodecatungostophosphoric acid (DTP) supported on K10 clay (20% w/w DTP/K10), dodecatungostophosphoric acid (DTP), partially substituted with Cs ($Cs_{2.5}H_{0.5}P_{12}W_{40}$) and supported on K10 clay (20% w/w Cs-DTP/K10) and ion exchange resins [8–20]. UDCaT-1 and UDCaT-5 are mesoporous solid superacids developed by us. In the case of acylation of ethers, 20% DTP/hexagonal mesoporous silica (HMS) and cation exchange resins were more active but deactivation was still a problem [18]. There is a dearth of systematic studies on acylation of aromatic ethers which deactivate solid acids in liquid phase reactions. For instance, synthesis of 2,5-dimethoxyacetophenone is achieved by the acylation of 1,4-dimethoxybenzene with $AlCl_3$ as catalyst [21–23]. It is used as a precursor for the CNS stimulant 2,5-dimethoxy-4-ethylphenethylamine (also called 2C-E). No report has so far appeared on the synthesis of 2,5-dimethoxyacetophenone using solid acid catalysts. The current work gives an insight into the acylation of 1,4-dimethoxybenzene with acetic anhydride as the acylating agent to get 2,5-dimethoxyacetophenone as the sole product including choice of catalyst, kinetic modeling and studies in catalyst deactivation and methods to avoid deactivation.

2. Experimental section

2.1. Chemicals and catalysts

All chemicals were A.R. grade and procured from reputed firms: 1,4-dimethoxybenzene (hydroquinone dimethyl ether) (Loba Chemie, Mumbai, India); acetic anhydride (Thomas Baker Chemicals Ltd., Mumbai); dodecatungstophoshporic acid (DTP), cesium chloride, zirconium oxychloride, ammonia solution (s.d. Fine Chemicals Pvt Ltd., Mumbai).

Cation exchange resins, Indion-125 (Ion Exchange (India) Ltd., Mumbai), Amberlyst-15 (Rohm and Hass, France) were available in the H^+ form and were dried at 120 °C before use.

Sulfated zirconia was prepared as reported earlier [24–26]. Twenty per cent w/w DTP/K-10 was prepared as given by us [27–29]. Twenty per cent w/w $Cs_{2.5}H_{0.5}PW_{12}O_{40}$/K-10 (abbreviated as Cs-DTP/K-10) was prepared as given in our earlier work [13,17]. UDCaT-1 and UDCaT-5 were prepared according to the method of Yadav and Goel [30] and Yadav and Murkute [31], respectively. All these catalysts have been well characterized and reported.

2.2. Reaction procedure

The reaction was carried out in a 100-ml capacity glass reactor of 4.5 cm i.d. equipped with four equally spaced baffles and six-pitched bladed turbine impeller of 1.5 cm diameter. The reaction temperature was maintained within ±0.5 °C by means of a thermostatic oil bath in which the reaction assembly was immersed. Standard experiments were carried out by taking 0.021 mol 1,4-dimethoxybenzene and 0.108 mol acetic anhydride at a temperature of 100 °C, and 0.05 g/cm^3 catalyst loading. All catalysts were dried at 120 °C for 5 h before use. The reaction mixture was allowed to reach the desired temperature and the initial sample was collected. Agitation was then commenced at a known speed. Samples were withdrawn periodically and analyzed by gas chromatography (GC). Typically acetic anhydride was taken in excess and the conversions were based on the limiting reactant, 1,4-dimethoxybenzene. The catalyst was separated by filtration, and the products confirmed by GC–MS.

2.3. Adsorption studies

Analysis of experimental data had suggested that it would be necessary to study adsorption of different species from liquid phase in the same reactor at the reaction temperature of 100 °C. The adsorption of reactants and products on the best catalyst, Indion-125 was studied. The adsorption studies were performed by taking the catalyst with a given substrate such as 1,4-dimethoxybenzene, 2,5-dimethoxyacetophenone, acetic anhydride and acetic acid in 1,4-dioxane as a solvent. A mixture of 1,4-dimethoxybenzene and 2,5-dimethoxyacetophenone in 1,4-dioxane along with catalyst was also used for the adsorption studies at 100 °C. The assembly was kept in a thermostatic oil bath at 100 °C and the contents were agitated at 1000 rpm. Clear samples were withdrawn periodically for analysis. The adsorbed quantity was found at each interval. The experiments were continued until there was no more adsorption of the substrate.

2.4. Analysis

Analysis of the reaction mixture was performed by GC (A Chemito, model 8510) by using FID and a stainless steel column (3.25 mm diameter and 2 m length) packed with 10% OV-17. Quantitative results were obtained by calibration using synthetic mixtures.

3. Results and discussions

3.1. Reaction scheme

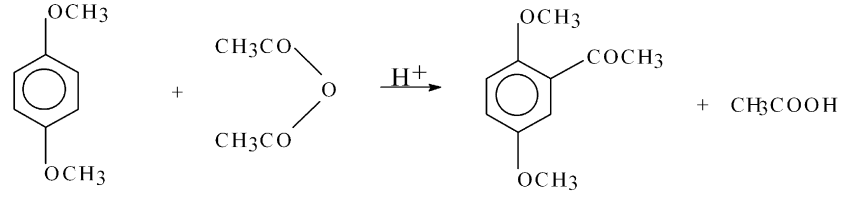

1,4- Dimethoxybenzene(A) Acetic anhydride(B) 2,5-Dimethoxyacetophenone (C) Acetic acid (D)

The analysis of reaction mixture showed that only the monoacylated product 2,5-dimethoxyacetophenone was formed.

3.2. Effect of different catalysts

1,4-Dimethoxybenzene is a bulky molecule and also an ether, which makes it a difficult molecule to acylate [6,18]. Based on the pore size distributions and acidity, various catalysts were screened for their efficacy and some of the most active catalysts for acylation reactions were selected. These included sulfated zirconia, 20% w/w DTP/K10, 20% w/w Cs-DTP/K10, UDCaT-1, UDCaT-5, Indion-125 and Amberlyst 15. Two temperatures were chosen, namely 100 °C without any solvent with excess of acetic anhydride and 90 °C with dichloroethane as a solvent (Fig. 1). Among these catalysts, Indion-125 and Amberlyst 15 were active. Twenty per cent w/w DTP/K-10, 20% w/w Cs-DTP/K10, sulfated zirconia, UDCaT-1 and UDCaT-5 were not active at 100 °C. These catalysts are superacidic in nature but get rapidly deactivated because of strong adsorption of the product. K10 is an acid treated montmorillonite clay with a surface area of 230 m^2/g and several pores in mesopore range. Sulfated zirconia has several pores in the mesopore range but has a wide pore size distribution [9,26]. UDCaT-1 has ordered mesoporosity and is a superacid [30,32]. UDCaT-5 possesses ordered mesoporosity [31,33] and is more superacidic than UDCaT-1. Heteropoly acids are not as strong as sulfated zirconia. UDCaT-5 did not show any measurable conversion at 100 °C when the temperature was raised to 130 °C using chlorobenzene as a solvent, the conversion was found to be 4.8%. This suggested that there was inhibition by reactants or products. However, cation exchange resins were found to be active at much lower temperatures. It was observed that the ion exchange resins Indion 125 and Amberlyst

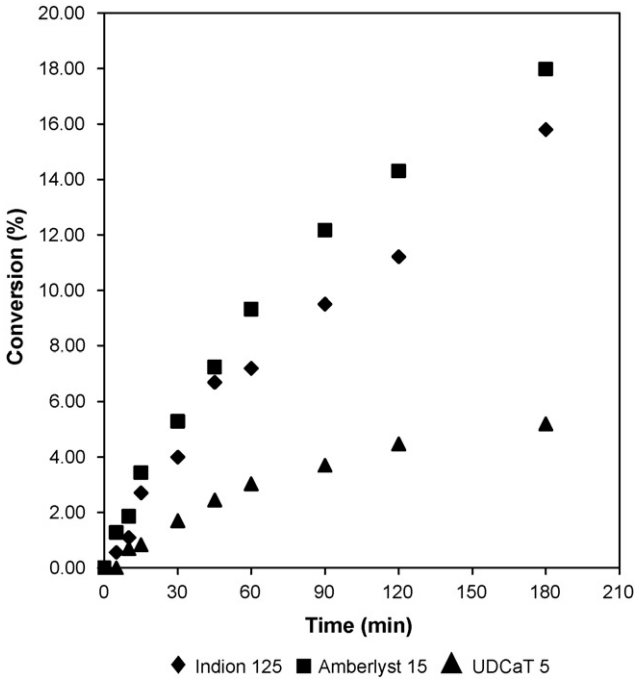

Fig. 1. The efficiency of different catalysts towards the acylation of 1,4-dimethoxybenzene. Reaction conditions: catalyst loading, 0.05 g/cm^3 of catalyst; speed of agitation, 1000 rpm; particle size, 500–600 μm; temperature, 100 °C except for UDCaT-5, for which the temperature was 130 °C with chlorobenzene as solvent; mole ratio of 1,4-dimethoxybenzene to acetic anhydride, 1:5.

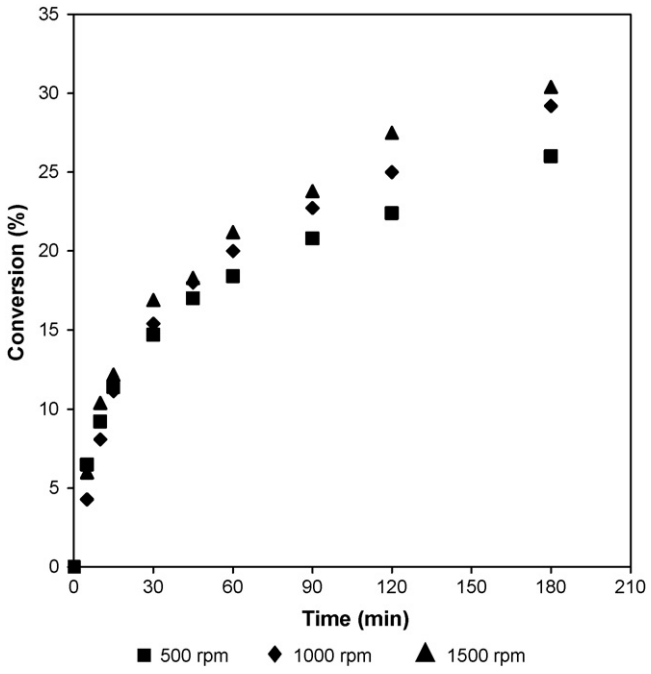

Fig. 2. Effect of speed of agitation on the conversion of 1,4-dimethoxybenzene. Reaction conditions: catalyst loading Indion-125, 0.05 g/cm^3; particle size, 500–600 μm; temperature, 100 °C; mole ratio of 1,4-dimethoxybenzene to acetic anhydride, 1:5.

15 were most efficient, giving conversions of 30.5% and 32.4%, respectively, after 1 h under the following reaction conditions: mole ratio of 1,4-dimethoxybenzene to acetic anhydride as 1:5, 20 ml 1,2-dichloroethane as solvent with a catalyst loading of 0.0452 g/cm^3 at 90 °C. Cation exchange resins are not as strong as other solid acids studied here and that helps in having weak adsorption of reactants and products. Since there is not much of a difference in the final conversions of Indion 125 and Amberlyst 15, further experiments were conducted with Indion 125. Both of them have similar cation exchange capacities. However, Indion 125 was available locally and hence all further studies were conducted with Indion 125.

3.3. Proof of absence of external mass transfer resistance

The effect of the speed of agitation was studied from 500 to 1500 rpm (Fig. 2). The conversions of 1,4-dimethoxybenzene were practically the same at 1000 and 1500 rpm suggesting that there was no resistance to the transfer of reactants to the exterior surface of the catalyst particle. All further experiments were carried out at 1000 rpm. A theoretical analysis of the effects of external mass transfer resistance is given to support this observation. Details of this theory for general slurry reactions are given elsewhere [24]. This is a typical solid–liquid slurry reaction involving the transfer of 1,4-dimethoxybenzene, the limiting reactant (A) and acetic anhydride (B) from the bulk liquid phase to the catalyst wherein transfer of reactants to the outer surface of the catalyst particle takes place, which is followed by intra-particle diffusion, adsorption, surface reaction and desorption. The influence of external solid–liquid mass transfer resistance must be ascertained before a true kinetic model could be developed. The reaction of 1,4-dimethoxyenzene (A) with acetic anhydride (B) produces 2,5-dimethoxyacetophenone (C) and acetic acid (D).

$$A + B \rightarrow C + D \quad (1)$$

At steady state, the rate of mass transfer per unit volume of the liquid phase (mol/cm^3 s) is given by:

$$R_A = k_{SL-A}\, a_p\{[A_o] - [A_s]\} \quad (2)$$

(rate of transfer of A from bulk liquid phase to external surface of the catalyst particle)

$$R_A = k_{SL-B}\, a_p\{[B_o] - [B_s]\} \quad (3)$$

(rate of transfer of B from the bulk liquid phase to the external surface of the catalyst particle)

$$R_A = r_{obs} \quad (4)$$

(observed rate of reaction within the catalyst particle).

Here the subscripts "o" and "s" denote the concentrations in bulk liquid phase and external surface of catalyst, respectively. Depending on the relative magnitudes of external resistance to mass transfer and reaction rates, different controlling mechanisms have been put forward [24]. When the external mass transfer resistance is negligible, then the following inequality holds:

$$\frac{1}{r_{obs}} \gg \frac{1}{k_{SL-A} a_p [A_0]} \quad (5)$$

$$\frac{1}{r_{obs}} \gg \frac{1}{k_{SL-B} a_p [B_0]} \quad (6)$$

The observed rate r_{obs} could be given by three types of models wherein the contribution of intra-particle diffusion resistance could be accounted for by incorporating the effectiveness factor η. These models are as follows:

(a) The Power Law model if there is very weak adsorption of reactant species.
(b) Langmuir–Hinshelwood–Hougen–Watson model.
(c) Eley–Rideal model.

According to Eqs. (5) and (6), it is necessary to calculate the rates of mass transfer of 1,4-dimethoxybenzene (A) and acetic anhydride (B) and to compare them with the overall rate of reaction. For a typical spherical particle, the particle surface area per unit liquid volume is given by

$$a_p = \frac{6w}{\rho_p d_p} \quad (7)$$

where w is the catalyst loading (g/cm^3) of liquid phase, ρ_p the density of particle (g/cm^3) and d_p is the particle diameter (cm). For this reaction, for the maximum catalyst loading used (0.1 g/cm^3) with a particle size (d_p) of 0.05 cm, in the current studies, $a_p = 20\ cm^2/cm^3$ liquid phase. The liquid phase diffusivity values of the reactant A denoted by D_{AB} was calculated by using the Wilke–Chang equation [33] at 100 °C as $3.95 \times 10^{-5}\ cm^2\ s^{-1}$. The corresponding value for reactant B was calculated as $1.89 \times 10^{-5}\ cm^2\ s^{-1}$ at 100 °C. The other reactant, acetic anhydride was used in excess such that it acted as the solvent. The solid–liquid mass transfer coefficients for A were calculated from the limiting value of the Sherwood number (e.g. $Sh_A = k_{SL-A}\ d_p/D_{AB}$) of 2. The actual Sherwood numbers are typically higher by order of magnitude in well-agitated systems but for conservative estimations a value of 2 is taken. The solid–liquid mass transfer coefficients k_{SL-A} and k_{SL-B} were obtained as 1.5808×10^{-3} cm/s and 7.56×10^{-4} cm/s, respectively. The initial rate of reaction was calculated from the conversion profiles. A typical initial rate of reaction was calculated as 2.00×10^{-7} mol/cm^3 s. Therefore, putting the appropriate values in Eqs. (5) and (6), i.e.

$$\frac{1}{r_{obs}} \gg \frac{1}{k_{SL-A} a_p [A_0]} \quad (8)$$

i.e. $4.98 \times 10^6 \gg 2.2592 \times 10^4$and

$$\frac{1}{r_{obs}} \gg \frac{1}{k_{SL-B} a_p [B_0]} \quad (9)$$

i.e. $4.98 \times 10^6 \gg 1.6534 \times 10^4$

The above inequality demonstrates that there is an absence of resistance due to the solid–liquid external mass transfer for both the species A and B and the rate may be either surface reaction controlled or intra-particle diffusion controlled. Therefore, the effects of catalyst loading at a fixed particle size and temperature were studied to evaluate the influence of intra-particle resistance.

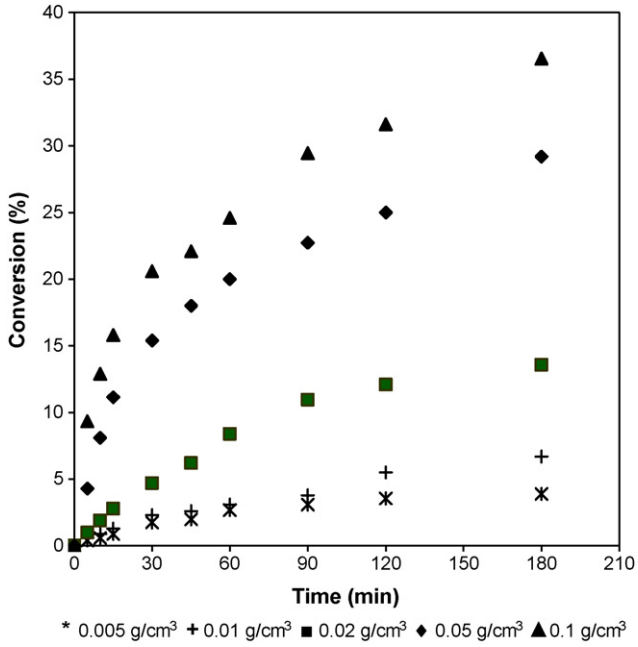

Fig. 3. Effect of catalyst loading on the conversion of 1,4-dimethoxybenzene. Reaction conditions: DMB, AA mole ratio 1:5; temperature, 100 °C; particle size, 500–600 μm; speed of agitation 1000 rpm.

3.4. Effect of catalyst loading

In the absence of external mass transfer resistance, the rate of reaction is directly proportional to catalyst loading based on the entire liquid phase volume. The catalyst loading was varied over a range of 0.005–0.1 g/cm^3 on the basis of total volume of the reaction mixture. Fig. 3 shows the effect of catalyst loading on the conversion of 1,4-dimethoxybenzene. The conversion increases with increasing catalyst loading, which is obviously due to the proportional increase in the number of active sites. All further experiments were carried out at 0.05 g/cm^3 of catalyst loading. As shown by Eqs. (1) and (2), at steady state, the rate of external mass transfer (i.e. from the bulk liquid phase in which A and B are located with concentration $[A_o]$ and $[B_o]$, respectively) to the exterior surface of the catalyst is proportional to a_p, the exterior surface area of the catalyst where the concentrations of A and B are $[A_s]$ and $[B_s]$, respectively. For a spherical spherical particle, a_p is also proportional to w, the catalyst loading per unit liquid volume as shown by Eq. (7). It is possible to calculate the values of $[A_s]$ and $[B_s]$.

For instance

$$k_{SL-A}\ a_p\{[A_o] - [A_s]\} = r_{obs} \text{ at steady state}$$
$$= 2.00 \times 10^{-7} mol/cm^3\ s$$

Thus, putting the appropriate values, it is seen that $[A_s] \approx [A_o]$, similarly $[B_s] \approx [B_o]$. Thus, any further addition of catalyst is not going to be of any consequence for external mass transfer.

3.5. Proof of absence of intra-particle resistance

The effect of particle size of the catalyst on the reaction rate was studied by taking three different particle size ranges

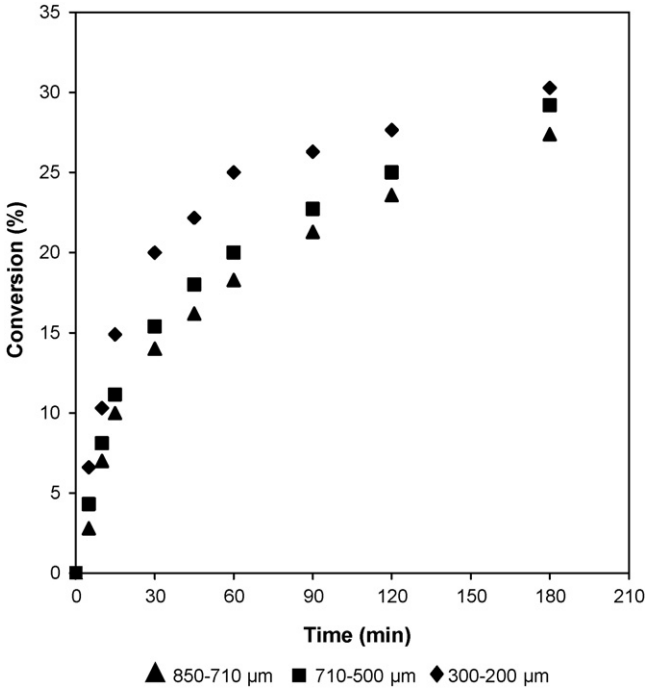

Fig. 4. Effect of particle size on the conversion of 1,4-dimethoxybenzene. Reaction conditions: mole ratio of 1,4-dimethoxybenzene to acetic anhydride, 1:5; Temperature, 100 °C; speed of agitation, 1000 rpm; catalyst loading, 0.05 g/cm^3 of Indion 125.

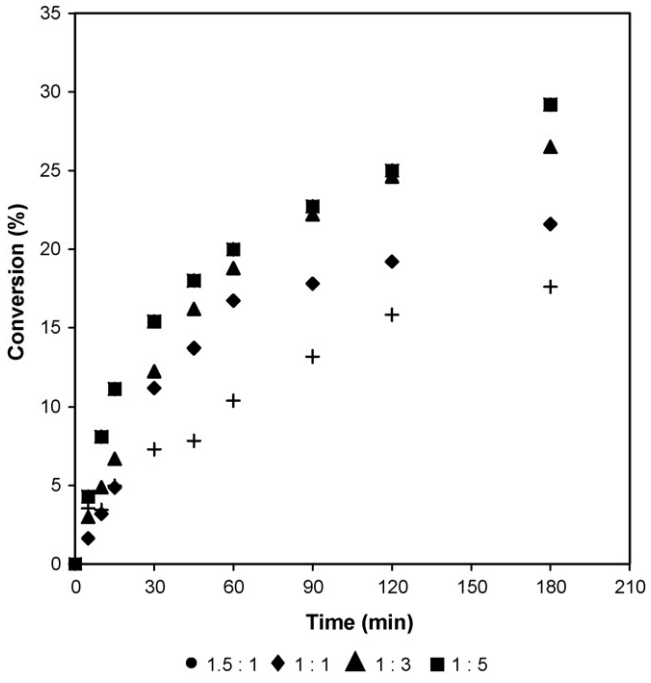

Fig. 5. Effect of mole ratio of 1,4-dimethoxybenzene to acetic anhydride on conversion of limiting reactant. Reaction conditions: catalyst loading, 0.05 g/cm^3 of Indion-125; speed of agitation 1000 rpm; particle size, 500–600 μm; temperature, 100 °C.

to assess the influence of intra particle resistance (Fig. 4). For an average particle size of 500 μm, there was no effect of particle size on the conversion of 1,4-dimethoxybenzene. The average particle diameter of the catalyst used in the reactions was 0.05 cm and thus a theoretical calculation was done based on the Wiesz–Prater criterion to assess the influence of intra-particle diffusion resistance [34]. According to the Wiesz–Prater criterion, the dimensionless parameter C_{wp} which represents the ratio of the intrinsic reaction rate to intra-particle diffusion rate, can be evaluated from the observed rate of reaction, the particle radius (R_p), effective diffusivity of the limiting reactant (D_e) and concentration of the reactant at the external surface of the particle.

(i) If $C_{wp} = r_{obs}\,\rho_p\,R_p^2/D_e[A_s] \gg 1$, (10a)

then the reaction is limited by severe internal diffusion resistance.

(ii) If $C_{wp} \ll 1$, (10b)

then the reaction is intrinsically kinetically controlled.

The effective diffusivity of 1,4-dimethoxybenzene (D_{e-A}) inside the pores of the catalyst was obtained from the bulk diffusivity (D_{AB}), porosity (ε) and tortuosity (τ) as 3.952×10^{-6} cm^2/s where $D_{e-A} = D_{AB}(\varepsilon/\tau)$. In the present case, the value of C_{wp} was calculated as 1.64×10^{-2} for the initial observed rate which is much less than 1 and therefore the reaction is intrinsically kinetically controlled. A further proof of the absence of the intra-particle diffusion resistance was obtained through the study of the effect of temperature and it will be discussed later.

3.6. Effect of mole ratio

The effect of mole ratio was studied at 1,4-dimethoxybenzene to acetic anhydride ratio of 1.5:1 to 1:5 (Fig. 5) under otherwise similar conditions. The conversion was found to increase with an increase in acetic anhydride concentration with respect to 1,4-dimethoxybenzene. The rate of reaction increases due to higher concentration of acetic anhydride on the surface of the catalyst. All the subsequent reactions were carried out with a mole ratio of 1:5 without any solvent, where acetic anhydride used in excess itself acts as a solvent.

3.7. Effect of temperature

The effect of temperature was studied in the range of 90–110 °C (Fig. 6). The conversion was found to increase substantially with increasing temperature, which suggested that the reaction was intrinsically kinetically controlled and the activation energy values should be determined to ascertain this observation.

3.8. Effect of the use of solvent

Reactions were performed using 1,2-dichloroethane as a solvent to study whether the use of solvent had any significant impact on the reaction rates. It was found that the use of solvent allowed the reaction to proceed at lower temperatures of 90 °C (Fig. 7). This effect, coupled with the adsorption studies, should yield an understanding of the reaction mechanism.

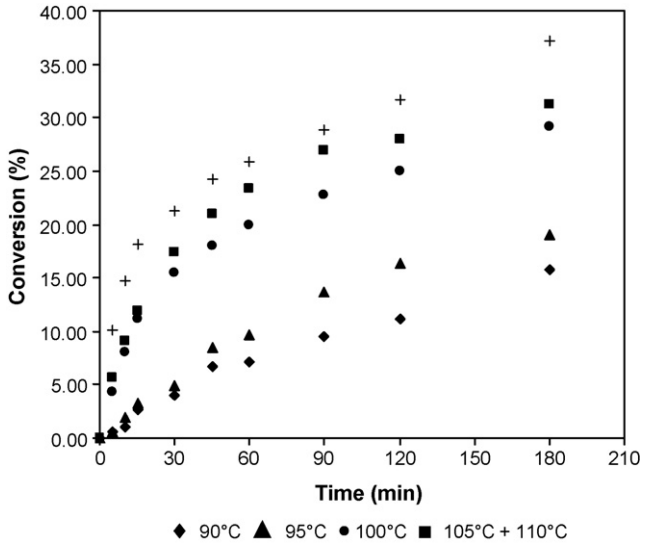

Fig. 6. Effect of temperature on the conversion of 1,4-dimethoxybenzene. Reaction conditions: catalyst loading, 0.05 g/cm^3 of Indion-125; speed of agitation, 1000 rpm, particle size, 500–600 μm; mole ratio of 1,4-dimethoxybenzene to acetic anhydride, 1:5.

3.9. Catalyst reusability studies

The reusability of the catalyst was studied by refluxing the used catalyst in methanol for 3 h in order to remove any adsorbed material from within the pores. It was dried at 110 °C after every use. The catalyst was reused twice at a mole ratio of 1,4-dimethoxybenzene to acetic anhydride of 1:5 (Fig. 8). There was a substantial loss in the activity. It thus appeared that the loss in activity could be due to one or many of the following reasons:

(i) Inhibition by either reactant molecules or product molecules which are strongly adsorbed on the active site. If adsorption constant of reactants are smaller than that of the product, then at higher conversions, more of product is likely to get adsorbed on the sites. This inhibition should be reversible and can be reduced by using higher temperatures.
(ii) Since the conversions are very high during the use of fresh catalyst, the bulkier product molecules could get strongly adsorbed at some critical pore junctions.
(iii) There is a physical trapping of product molecules in critical pore junctions rendering some pore networks inaccessible to the reactants.

A physical depiction of these arguments is provided in Fig. 9.

To find out the cause of the deactivation, adsorptions studies were undertaken. It was thought desirable to measure the adsorption equilibrium constant and adsorption rate constants from batch slurry reactors [35]. In this method, an adsorbate was added to a slurry containing adsorbate or catalyst particles at time equal to zero. The concentration of the adsorbate was then observed as a function of time. From these transient data, it was possible to calculate adsorption and transport parameters such as solid–liquid mass transfer coefficient (k_{SL}), effective diffusivity (D_e) in the liquid filled pores [35] (Figs. 10–16).

At high catalyst loading and lower concentration of adsorbate, the adsorption process is linear, and the rate of adsorption

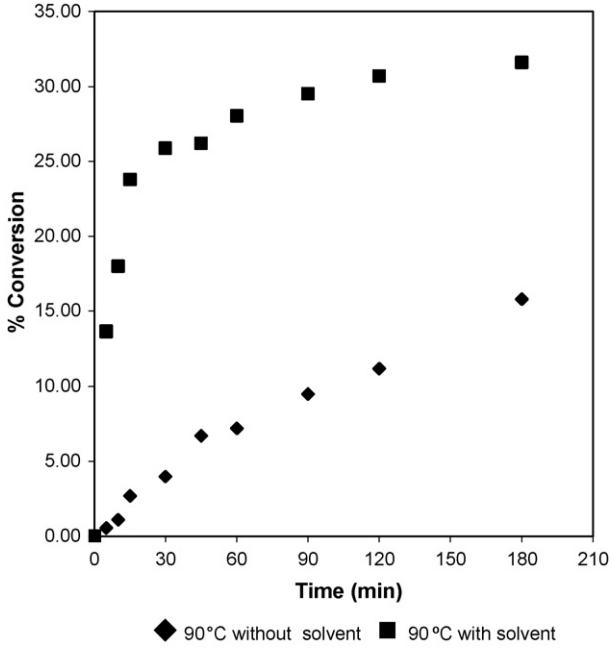

Fig. 7. The effect of the use of solvent. Reaction conditions: (without solvent) catalyst loading: 0.05 g/cm^3 of Indion-125; speed of agitation, 1000 rpm; particle size, 500–600 (m; mole ratio of 1,4-dimethoxybenzene to acetic anhydride 1:5. (With solvent) mole ratio of 1,4 dimethoxybenzene to acetic anhydride, 1:5; solvent, 10 ml EDC (total reaction volume 25 ml); catalyst loading 0.05 g/cc of Indion 125; speed of agitation, 1000 rpm; particle size, 500–600 (m.

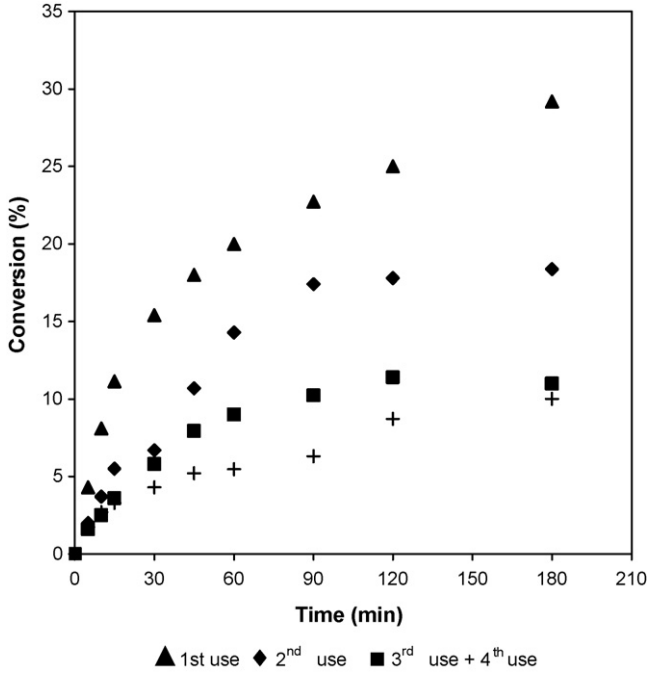

Fig. 8. Effect of catalyst reuse on the conversion of 1,4-dimethoxybenzene. Reaction conditions: catalyst loading, 0.05 g/cm^3 of Indion-125; speed of agitation, 1000 rpm; particle size 500–600 μm; temperature, 100 °C; mole ratio of 1,4-dimethoxybenzene to acetic anhydride, 1:5.

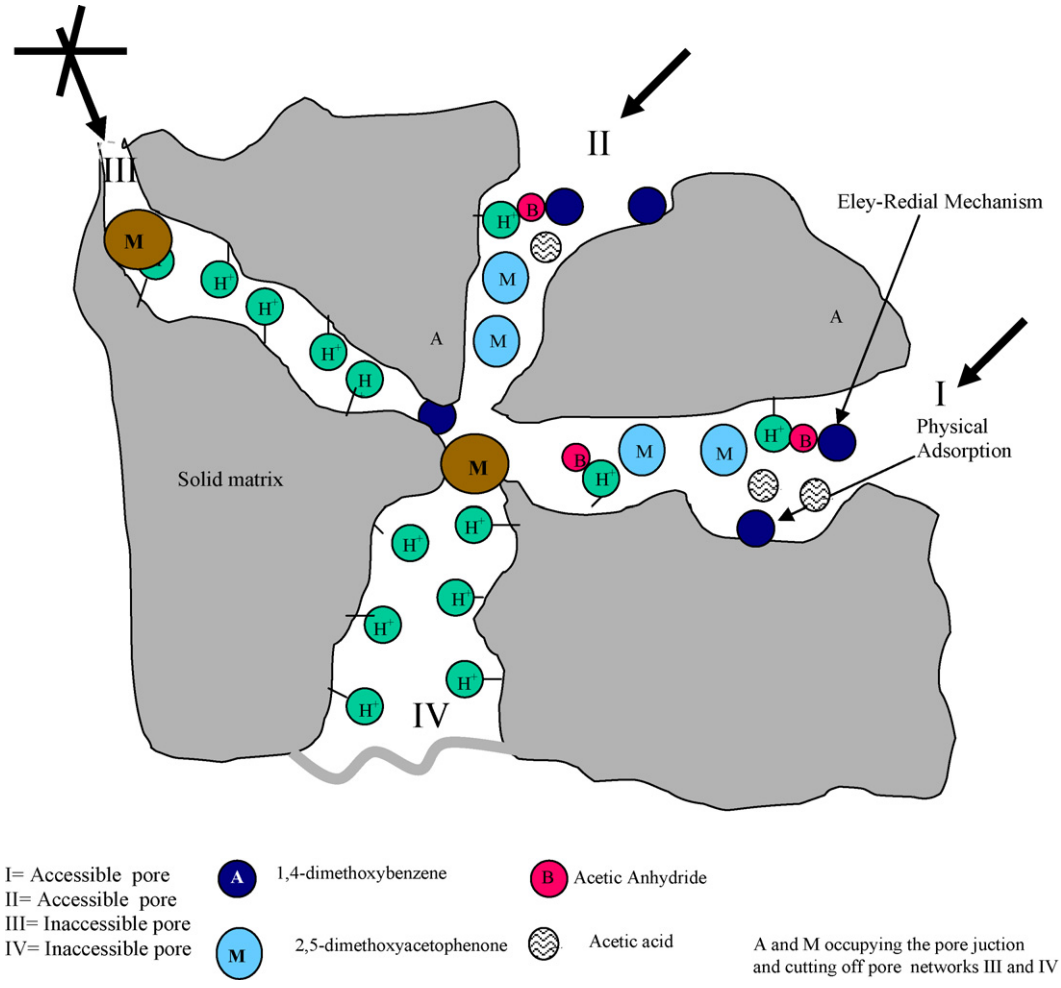

Fig. 9. Schematic of catalyst deactivation mechanism.

is given by,

$$k_{ad} = k_A \left(\frac{C_A - S_A}{K'_A} \right) \tag{11}$$

where S_A is the surface concentration of adsorbed A, mol/g; C_A, concentration of A in the liquid phase, mol/cm^3; k_{ad}, adsorption constant, cm^3/(g cat/s); K_A, adsorption equilibrium constant, $K'_A = K_A C_t$ cm^3/g, $k_A = k_{ad} C_t$, where C_t is the total concent.ration of active sites, mol/g.

The concentration profile of the adsorbent in the liquid phase is given by the following equation:

$$\frac{C_{AL}}{C_{ALf}} = \frac{1}{(1 + wK'_A)} + \frac{wK'_A}{(1 + wK'_A)} \exp \left[\frac{(1 + wK'_A) k_{SL} a_p t}{wK'_A} \right] \tag{12}$$

where C_{AL} is the concentration of species A in the liquid phase at any time t and C_{ALf} is the final concentration at infinite time.

The parameter K'_A can be obtained from batch experiments.

$$K'_A = \frac{1}{w} \left[\frac{C_{ALi}}{C_{ALf}} - 1 \right] \tag{13}$$

where C_{ALi} is the initial concentration of A in the liquid, gmol/cm^3; C_{ALf}, final concentration of A in the liquid at $t = \infty$, and w = catalyst loading, g/cm^3 of liquid.

Thus, K'_A can be found.

The adsorption constant K_A (cm^3/mol) is obtained from the following equation:

$$K_A = \frac{K'_A}{((C_{ALi} - C_{ALf})/w)} \tag{14}$$

The change in concentration of a compound under reaction conditions was studied first in isolation. Subsequently, the simultaneous adsorption of the reactants in absence of acetic anhydride was studied.

From the experimental data, the adsorption constants for dimethoxybenzene turn out to be 850.6 cm^3/mol (individually) and 858.2 cm^3/mol (for simultaneous adsorption with dimethoxyacetophenone). Thus, the values are found to be in good agreement. The value for acetic anhydride is 319.9 cm^3/mol. Adsorption constants for dimethoxtacetophenone were 885.6 cm^3/mol (in isolation) and 1424.5 cm^3/mol (on simultaneous adsorption with dimethoxybenzene).

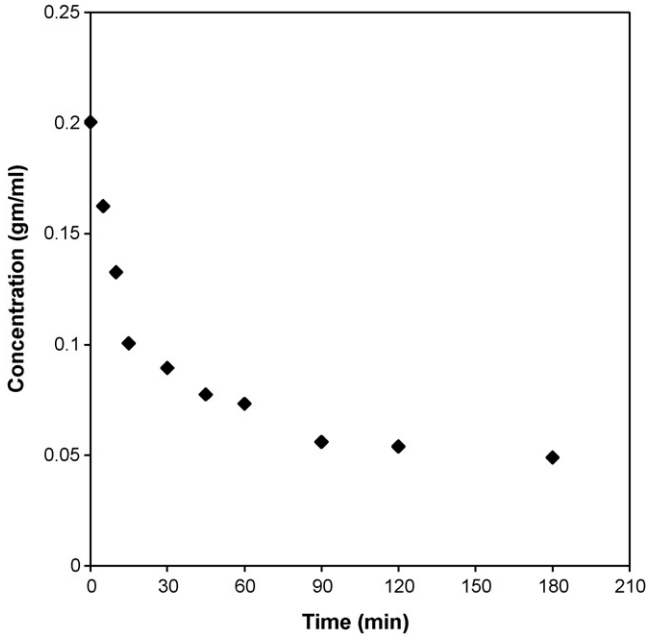

Fig. 10. Adsorption of 1,4-dimethoxybenzene on Indion-125. Conditions: 3.0048 g (0.021 mol) 1,4-dimethoxybenzene; 11 ml 1,4-dioxan as solvent; catalyst loading, 0.05 g/cc (0.75 g in 15 cc); temperature, 100 °C; speed of agitation, 1000 rpm.

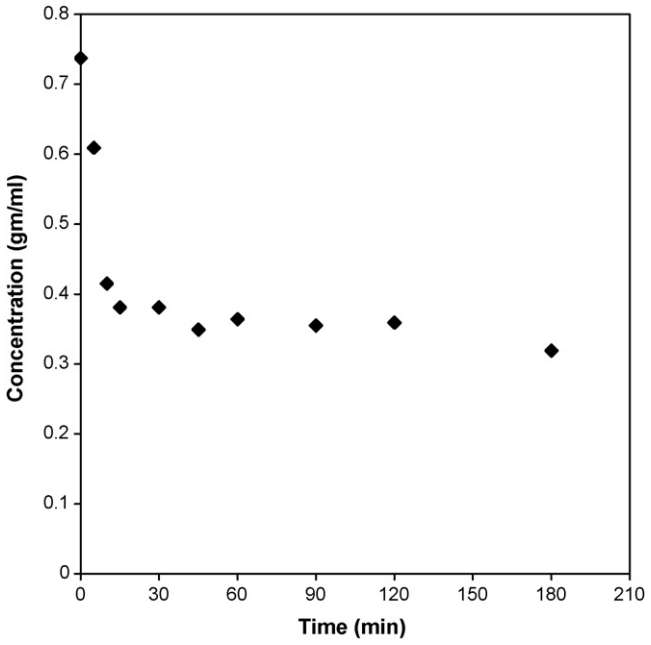

Fig. 12. Adsorption of acetic anhydride on Indion-125. Conditions: 11.06 g (0.108 mol) acetic anhydride; catalyst loading, 0.05 g/cc (0.75 g in 15 cc); temperature, 100 °C; speed of agitation, 1000 rpm.

According to the Eq. (12) a plot of $\ln[(C_{AL}/C_{ALf} - 1/(1 + wK'_A)]$ versus time gives a slope of $((1 + wK'_A)k_{SL}a_p)/wK'_A$ from which $k_{SL}a_p$ can be found out. The value for k_{SL} by this procedure is (from Fig. 15) 2.89×10^{-3} cm/s. This compares favorably with the value of $k_{SL} = 1.5808 \times 10^{-3}$ cm/s obtained by using Wilke Chang correlation [33].

4. Reaction mechanism and kinetics

From the calculated values of mass transfer rates of A and B, initial observed rate, it is evident that the rate is independent of the external mass transfer effects. A preliminary calculation of activation energy from the initial rate data showed that

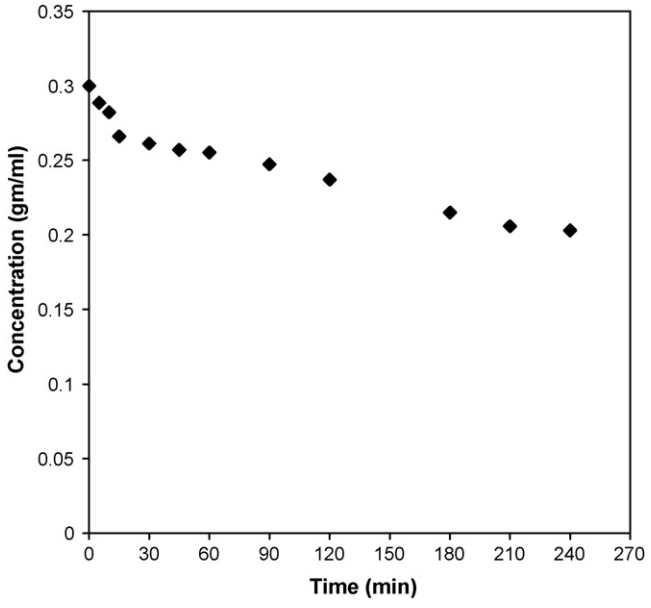

Fig. 11. Adsorption of product 2,5-dimethoxyacetophenone on Indion-125. Conditions: 4.556 g (0.025 mol) 2,5-dimethoxyacetophenone; 10 ml 1,4-dioxan as solvent; catalyst loading, 0.05 g/cc (0.75 g in 15 cc); temperature 100 °C; speed of agitation, 1000 rpm.

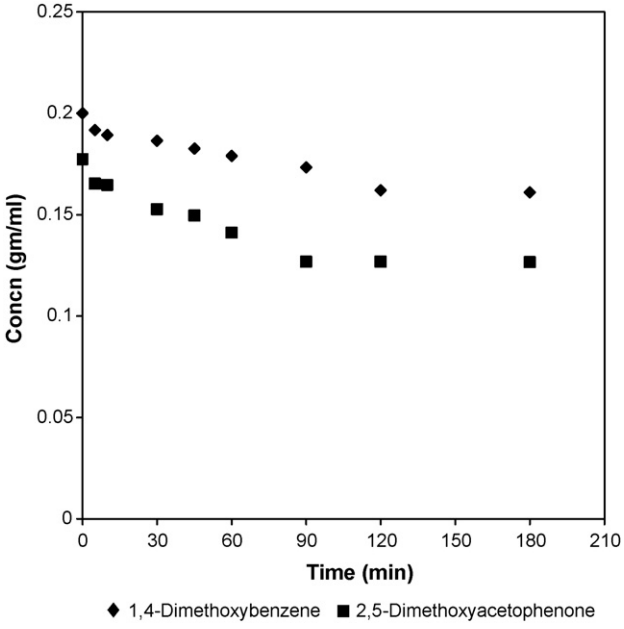

Fig. 13. The simultaneous adsorption of 1,4-dimethoxybenzene and 2,5-dimethoxyacetophenone in the absence of acetic anhydride. Conditions: 0.021 mol 1,4-dimethoxybenzene; 0.0124 mol 2,5-dimethoxyacetophenone in 1,4-dioxan at 100 °C; 0.05 g/cc of Indion-125.

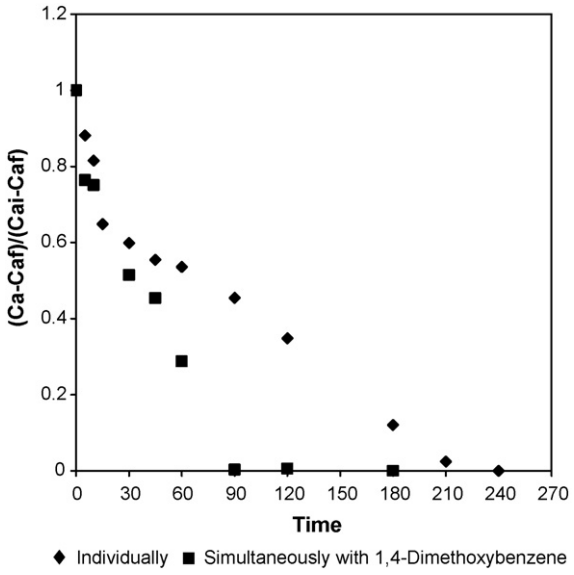

Fig. 14. The adsorption of 2,5-dimethoxyacetophenone on Indion 125. Conditions: catalyst loading, 0.05 g/cc; temperature, 100 °C.

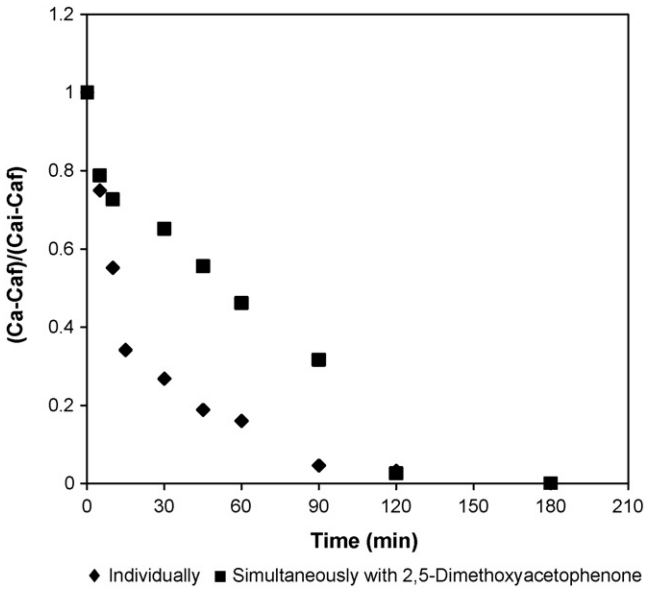

Fig. 15. The adsorption of 1,4-dimethoxybenzene on Indion 125. Conditions: catalyst loading, 0.05 g/cc; temperature, 100 °C.

the reaction was not affected by intra-particle resistance. Thus, the reaction could be controlled by one of the following steps, namely: (a) adsorption, (b) surface reaction or (c) desorption. Therefore, for further development of model, a study of the actual reaction mechanism was undertaken.

Proposed model:

The above studies can now be used to develop a mechanistic model for the reaction.

$$(CH_3CO)_2O \xrightarrow{H^+} {}^+COCH_3 + CH_3COOH$$

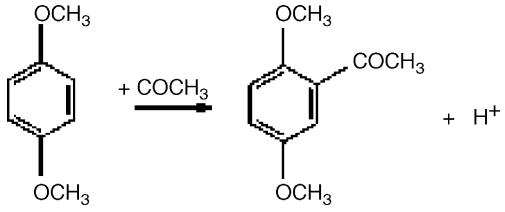

Chemisorption of acetic anhydride

$$B + S \underset{k'_A}{\overset{k_A}{\rightleftharpoons}} BS + C \tag{15}$$

The net rate of chemisorption is given by the following mass balance:

$$-r_A = k_A C_B C_S - k'_A C_{BS} C_C \tag{16}$$

which approximates to zero at equilibrium.

From which,

$$C_{BS} = K_A \frac{C_B C_S}{C_C} \tag{17}$$

where K_A is adsorption equilibrium constant $= k_A/k'_A$

Surface reaction:

$$A + BS \xrightarrow{k_{SR}} MS \tag{18}$$

where k_{SR} is the reaction rate constant, with the assumption that the forward reaction is the rate determining step.

The rate of reaction of A is given by:

$$\frac{-dC_A}{dt} = k_{SR} C_A C_{BS} a \tag{19}$$

The activity of the catalyst is given by:

$$a = \frac{-r_A}{-r_{A(fresh)}} = \frac{\text{rate of A at any time t}}{\text{rate of reaction A with fresh catalyst}} \tag{20}$$

Rate of deactivation is assumed to be first order ($d = 1$),

$$\frac{-da}{dt} = k_{DE}\, a \tag{21}$$

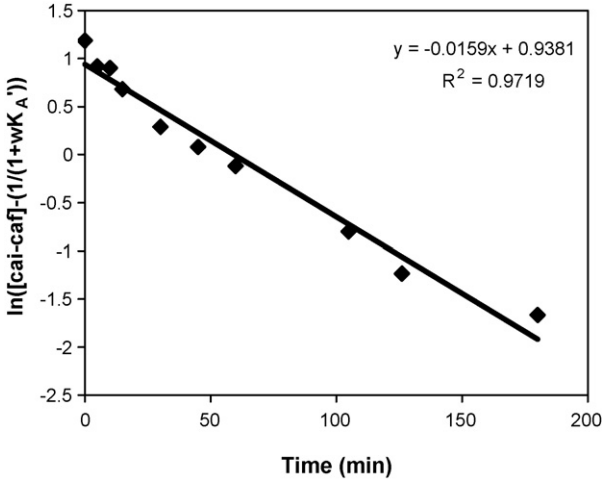

Fig. 16. The adsorption of 1,4-dimethoxybenzene on Indion 125. Conditions: catalyst loading, 0.05 g/cc; temperature, 100 °C; k_{SL} from above graph $= 2.89 \times 10^{-3}$ cm/s.

Integration of Eq. (21),

$$a = a_o \exp(-k_{DE}t) = \exp(-k_{DE}t) \tag{22}$$

where, $a_o = 1$ = initial activity

Rate of desorption of the product, 2,5-dimethoxyacetophenone,

$$MS \underset{k'_{D1}}{\overset{k_{D1}}{\rightleftharpoons}} M + S \tag{23}$$

The net rate of desorption of the product M,

$$-r_{D1} = k_{D1}C_{MS} - k'_{D1}C_M C_S, \tag{25}$$

which approximates zero at equilibrium (quasi-equilibrium)

Therefore,

$$C_{MS} = K_{D1}C_M C_S \tag{26}$$

where K_{D1} is desorption equilibrium constant for the product, $K_{D1} = k_{D1}/k'_{D1}$

Desorption of acetic acid (C):

$$CS \underset{k'_{D2}}{\overset{k_{D2}}{\rightleftharpoons}} C + S \tag{27}$$

The net rate of desorption of acetic acid by mass balance is given by:

$$-r_{D2} = k_{D2}C_{CS} - k'_{D2}C_M C_S \tag{28}$$

which approximates zero at equilibrium (quasi-equilibrium), leading to:

$$C_{CS} = K_{D2}C_C C_S \tag{29}$$

where $K_{D2} = k_{D2}/k'_{D2}$ = the desorption equilibrium constant

After substituting for C_{BS} in the rate equation,

$$\frac{-dC_A}{dt} = k_{SR}\frac{C_A K_A C_B C_S}{C_C}a \tag{30}$$

$$\frac{-dC_A}{dt} = (k_{SR}K_A)\frac{C_A C_B C_S}{C_C}\exp(-k_{DE}t) \tag{31}$$

where the value of a has been substituted from Eq. (21)

The total site balance is as follows:

$$C_{total} = w = C_{BS} + C_{MS} + C_{CS} \tag{32}$$

where w is the catalyst loading.

From Eqs. (17), (26) and (29),

$$C_{total} = w = K_A\frac{C_B C_S}{C_C} + K_{D1}C_M C_S + K_{D2}C_C C_S \tag{33}$$

Thus,

$$C_S = \left(\frac{w}{(K_A C_B)/(C_C) + K_{D1}C_M + K_{D2}C_C}\right) \tag{34}$$

Therefore,

$$\frac{-dC_A}{dt} = k_{SR}K_A C_A C_B \exp(-k_{DE})t \times \left\{\frac{w}{(K_A C_B)/(C_C) + K_{D1}C_M + K_{D2}C_C}\right\} \tag{35}$$

Now, in terms of fractional conversions of X_A,

$$C_A = C_{A0}(1 - X_A) \tag{36}$$

$$C_B = C_{B0}(1 - X_B) = C_{A0}(M - X_A) \tag{37}$$

$$C_C = C_M = C_{A0}X_A \tag{38}$$

where $C_{B0}/C_{A0} = M$, initial mole ratio of acetic anhydride to 1,4-dimethoxybenzene

$$\frac{-dC_A}{dt} = C_{A0}\frac{dX_A}{dt} \tag{39}$$

Substituting the above equations in the rate equation, the rate equation takes the form

$$\frac{dX_A}{dt} = k_{SR}K_A w(M - X_A)(1 - X_A)\exp(-k_{DE}t) \times \left\{\frac{1}{K_A(M - X_A) + [K_{D1} + K_{D2}]C_{A0}X_A^2}\right\} \tag{40}$$

The Eq. (41) is also amenable to analytical solution, the result being

$$-K_A \ln(1 - X_A) + C_{A0}\left(\frac{1}{K_{A1}} + \frac{1}{K_{A2}}\right) \times \left\{X_A + \frac{M^2}{M-1}\ln(M - X_A) - \frac{1}{M-1}\ln(1 - X_A) - \frac{M^2}{M-1}\ln M\right\} = \frac{k_{SR}K_A w\exp(-k_{DE}t)}{-k_{DE}} \tag{41}$$

Eq. (41) can be manipulated to get the following form:

$$\ln\left[1 - \frac{k_{DE}}{K_A k_{SR} w}\left(-K_A \ln(1 - X_A) + C_{A0}\left(\frac{1}{K_{A1}} + \frac{1}{K_{A2}}\right) \times \left\{X_A + \frac{M^2}{M-1}\ln(M - X_A) - \frac{1}{M-1}\ln(1 - X_A) - \frac{M^2}{M-1}\ln M\right\}\right)\right] = -k_{DE}t \tag{42}$$

In the above equation the desorption constants have been replaced by adsorption constants ($K_{A1} = 1/K_{D1}$; $K_{A2} = 1/K_{D2}$)

Two approaches were adopted. Eq. (40) was subjected to non linear regression, to obtain the values of various parameters, on the basis of experimental rates and conversions. At the same time, Eq. (42), a modified form of the analytical solution was used to estimate values of k_{DE} and k_{SR}, using experimentally determined values of adsorption constants. This was done in the following manner. Fig. 17 shows the plot as per Eq. (42).

Knowing the experimental rates and conversions with respect to time, all the rate constants and adsorption constants were calculated by applying non linear regression to Eq. (40) using polymath 5.1. The best-fit values obtained are tabulated in Table 1. These values were then used to generate simulated conversion values. Eq. (42) was integrated numerically using Euler's method and a step size of integration of 0.5. Limits imposed on the integration were time varying from 0 to 180 min, with initial conversion X_A as zero. Simulated values of conversion so

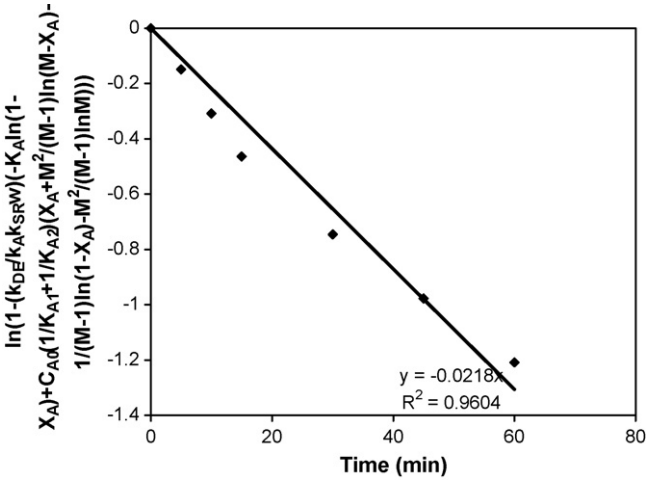

Fig. 17. Validation of the model using experimental data and Eq. (42). Reaction conditions: temperature, 100 °C; catalyst loading, 0.05 g/cc of Indion 125; speed of agitation, 1000 rpm; particle size, 500 to 600 μm; mole ratio of acetic anhydride to dimethoxybenzene, 1:5.

obtained were compared with experimental values, as shown in Fig. 18.

Experimentally obtained values of adsorption constants were used in Eq. (42). From the experimental data, the adsorption constants for dimethoxybenzene (K_A) was determined as 850.6 cm^3/mol. Adsorption constants for dimethoxtacetophenone (K_{A1}) and acetic acid were calculated as 885.6 cm^3/mol and 963 cm^3/mol, respectively.

Eq. (42) was subjected to nonlinear regression using polymath 5.1, the parameters to be fitted being k_{DE} and k_{SR}. The value of k_{DE} obtained by this procedure was 0.022. The value for k_{SR} obtained was 0.16 (Fig. 17).

The values of k_{DE} and k_{SR} obtained using the two procedures are in good agreement (Table 2). Thus, these two approaches acted as a check for internal consistency. Thus, the proposed model is validated. Plots were made for reactions carried out at different temperatures to calculate rate constants. The Arrhenius plots are shown in (Figs. 19 and 20) to get the activation energy value for reaction and deactivation as 27.97 and 13.45 kcal/mol, respectively. For an average particle size of 500 μm, and at a speed of agitation beyond 1000 rpm, with 1,4-dimethoxybenzene to acetic anhydride mole ratio of 1:5, there was no mass transfer effect at 100 °C. These results show that the reaction is intrinsically kinetically controlled. Besides, the

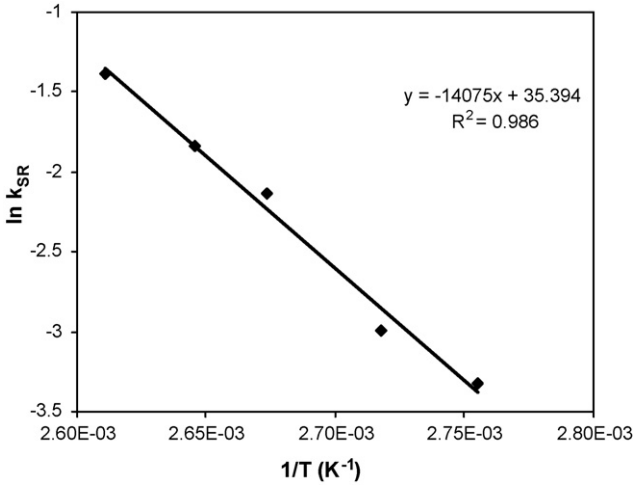

Fig. 18. Comparison of the experimental and predicted fractional conversions.

Table 2
Comparison of k_{DE} and k_{SR} values obtained by (1) nonlinear regression applied to Eq. (38) and (2) nonlinear regression applied to the analytical solution, Eq. (40)

	k_{DE}	k_{SR}
From Eq. (40)	0.02	0.14
From Eq. (42), using experimental values of adsorption constants	0.022	0.16

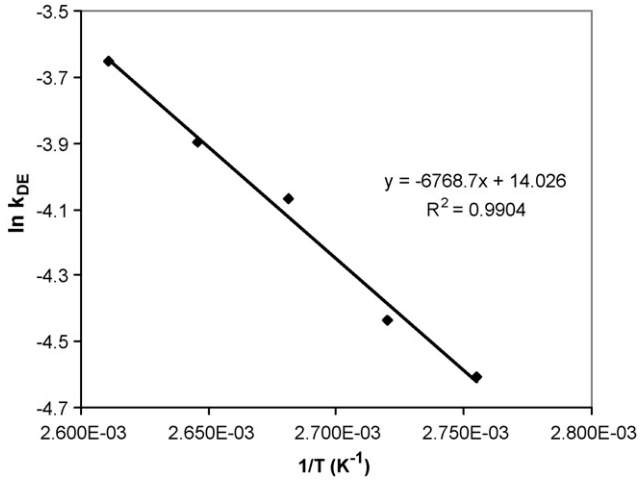

Fig. 19. Arrhenius Plot of ln k_{SR} vs. 1/T. Reactions conditions: catalyst loading, Indion-125 0.05 g/cm^3; speed of agitation, 1000 rpm; particle size, 500–600 μm; mole ratio of dimethoxybenzene to acetic anhydride, 1:5.

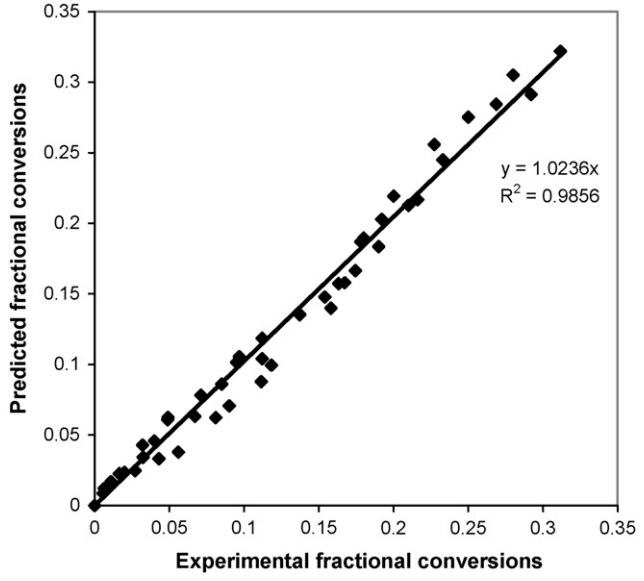

Fig. 20. Arrhenius Plot of ln k_{DE} vs. 1/T. Reactions conditions: catalyst loading, Indion-125 0.05 g/cm^3; speed of agitation, 1000 rpm; particle size, 500–600 μm; mole ratio of dimethoxybenzene to acetic anhydride, 1:5.

deactivation of resins could be overcome by using higher temperature. Since the cation exchange resins have an upper and safer limit of 120 °C, these data were used to predict the conversions at 120 °C. The catalyst was tested at this temperature and reused five times without much loss in activity from run to run. The deactivation of ion exchange resins can be overcome by choosing a higher temperature of 120 °C and a mole ratio of 1:5, when the conversion of reaches 60% and recycle of the unreacted starting materials could be achieved. When chlorobenzene is used as a solvent, the deactivation is totally overcome. However, it introduces, additional separation step.

5. Conclusion

The acylation of 1,4-dimethoxybenzene was conducted by using acetic anhydride as the acylating agent over a number of catalysts of different acidities and pore size distributions such as sulfated zirconia, UDCaT-1, UDCaT-5, 20% w/w DTP/K10, 20% w/w Cs-DTP/K10 and ion exchange resins. Amberlyst1-5 and Indion-125 were found to be the most active catalysts. The effect of various parameters on the reaction rate was studied with Indion-125. The optimum conditions were: 1,4-dimethoxybenzene to acetic anhydride mole ratio of 1:5, 100 °C, catalyst loading of 0.05 g cm^{-3}. A systematic study was undertaken to understand the reaction mechanism and catalyst functioning. The catalyst is deactivated over repeated use at lower temperatures. The adsorption of reactants and products was studied both individually and simultaneously. The experimental data so generated were used to develop a model. The model fits the experimental data very well. The deactivation could be overcome by using a temperature of 120 °C at a mole ratio of 1:5 of 1,4-dimethoxybenzene to acetic acid.

Acknowledgements

G.D.Y. acknowledges support from the Darbari Seth Endowment. K.P.P. acknowledges the University Grants Commission (UGC) for awarding the Junior Research Fellowship.

References

[1] G.A. Olah, Friedel-Crafts Chemistry, Wiley Interscience, New York, 1973.
[2] A. Cybulski, J. Moulijn, M.M. Sharma, R.A. Sheldon, Fine Chemicals Manufacture Technology and Engineering, first ed., Elsevier, Amsterdam, The Netherlands, 2001.
[3] B.M. Choudary, M. Sateesh, M.L. Kantam, K.V. Ram Prasad, Appl. Catal. 171 (1998) 155.
[4] M. Spagnol, L. Gilbert, D. Alby, Ind. Chem. Libr. 8 (1996) 29.
[5] P. Metivier, in: R.A. Sheldon, H. van Bekkum (Eds.), Fine Chemicals through Heterogeneous Catalysis, Wiley, Weinheim, Toronto, 2001, p. 161.
[6] P. Moreau, A. Finiels, P. Meric, J. Mol. Catal. 154 (2000) 185.
[7] T. Raja, A.P. Singh, A.V. Ramaswamy, A. Finiels, P. Moreau, Appl. Catal. 211 (2001) 31.
[8] G.D. Yadav, M.S. Krishnan, Chem. Eng. Sci. 54 (1999) 4189–4197.
[9] G.D. Yadav, J.J. Nair, Micro. Meso. Mater. 33 (1999) 1–48.
[10] G.D. Yadav, A.A. Pujari, Green Chem. 1 (2) (1999) 69–74.
[11] G.D. Yadav, N.S. Asthana, Ind. Eng. Chem. Res. 41 (2002) 5565–5575.
[12] G.D. Yadav, A.V. Joshi, Clean Tech. Environ. Policy 4 (3) (2002) 157–164.
[13] G.D. Yadav, N.S. Asthana, V.S. Kamble, Appl. Catal. A: Gen. 240 (2003) 53–69.
[14] G.D. Yadav, M.S.M.M. Rahuman, Ultrasound Sonochem. 10 (3) (2003) 135–138.
[15] G.D. Yadav, H.G. Manyar, Micro. Meso. Mater. 63 (1–2) (2003) 85–96.
[16] S.P. Patil, G.D. Yadav, Comput. Biol. Chem. 27 (2003) 393–404.
[17] G.D. Yadav, N.S. Asthana, V.S. Kamble, J. Catal. 217 (1) (2003) 88–99.
[18] G.D. Yadav, S.P. Nalawade, Chem. Eng. Sci. 58 (2003) 2573–2585.
[19] G.D. Yadav, N.S. Asthana, S.S. Salgaonkar, Clean Tech. Environ. Policy 6 (2004) 105–113.
[20] G.D. Yadav, R.D. Bhagat, J. Mol. Cat. A: Chem. 235 (1–2) (2005) 98–107.
[21] Ber., 37 (1904) 3993.
[22] Ber., 38 (1905) 789.
[23] C. Kuroda, Sci. Papers Inst. Phy. Chem. Res. (Tokyo) 18 (1932) 51.
[24] P.S. Kumbhar, G.D. Yadav, Chem. Eng. Sci. 44 (1989) 2535.
[25] G.D. Yadav, T.S. Thorat, Ind. Eng. Chem. Res. 35 (1996) 721–732.
[26] P.S. Kumbhar, V.M. Yadav, G.D. Yadav, in: D.E. Layden (Ed.), Chemically Modified Oxide Surfaces, Gordon and Breach, New York, 1989.
[27] G.D. Yadav, N. Kirthivasan, J. Chem. Soc. Chem. Commun. 2 (1995) 203–204.
[28] G.D. Yadav, N. Kirthivasan, Appl. Catal. A: Gen. 154 (1–2) (1997) 29–53.
[29] G.D. Yadav, V.V. Bokade, Appl. Catal. A: Gen. 147 (2) (1996) 299–315.
[30] G.D. Yadav, P.K. Goel, Clean Tech. Environ. Policy 4 (3) (2002) 165–170.
[31] G.D. Yadav, A.D. Murkute, J. Catal. 224 (2004) 218–223.
[32] G.D. Yadav, M.S. Krishnan, A.A. Pujari, N.S. Doshi, M.S.M. Mujeebur Rahuman, US Patent 6,204,424 (2001);
G.D. Yadav, A.D. Murkute, Langmuir 20 (2004) 11607.
[33] R.C. Reid, M.J. Prausnitz, T.K. Sherwood, The Properties of Gases and Liquids, third ed., McGraw-Hill, New York, 1977.
[34] H.S. Fogler, Elements of Chemical Reaction Engineering, Prentice-Hall, New Delhi, 1995.
[35] P.A. Ramchandran, R.V. Chaudhari, Three Phase Catalytic Reactors, Gordon Breach, New York, 1983.